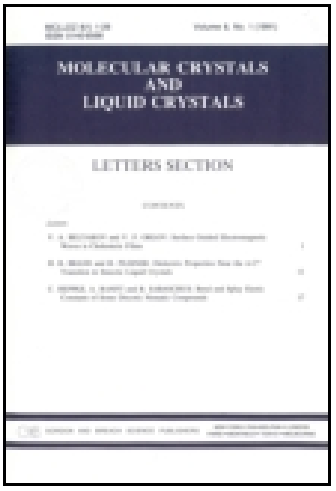

Molecular Crystals and Liquid Crystals
Publication details, including instructions for authors and subscription information:
http://www.tandfonline.com/loi/gmcl20

Morphology of Silver Nanoparticles in the Micelle-Forming Block Copolymers

S. V. Fedorchuk [a] , T. B. Zheltonozhskaya [a] , Yu. P. Gomza [b] , D. O. Klymchuk [c] & L. R. Kunitskaya [a]

[a] Kiev National University of Taras Shevchenko, Faculty of Chemistry, Department of Macromolecular Chemistry , 60 Vladimirskaya St, 01033 Kiev , Ukraine

[b] Institute for Macromolecular Chemistry , National Academy of Sciences of Ukraine , 48 Kharkovskoye Shosse, 02160 , Kiev , Ukraine

[c] Institute of Botany , National Academy of Sciences of Ukraine , 2 Tereschenkovskaya St., 01601 , Kiev , Ukraine

Published online: 28 Mar 2014.

To cite this article: S. V. Fedorchuk , T. B. Zheltonozhskaya , Yu. P. Gomza , D. O. Klymchuk & L. R. Kunitskaya (2014) Morphology of Silver Nanoparticles in the Micelle-Forming Block Copolymers, Molecular Crystals and Liquid Crystals, 590:1, 172-178, DOI: 10.1080/15421406.2013.874213

To link to this article: http://dx.doi.org/10.1080/15421406.2013.874213

Mol. Cryst. Liq. Cryst., Vol. 590: pp. 172–178, 2014

ISSN: 1542-1406 print/1563-5287 online
DOI: 10.1080/15421406.2013.874213

Taylor & Francis
Taylor & Francis Group

Morphology of Silver Nanoparticles in the Micelle-Forming Block Copolymers

S. V. FEDORCHUK,[1,*] T. B. ZHELTONOZHSKAYA,[1]
YU. P. GOMZA,[2] D. O. KLYMCHUK,[3]
AND L. R. KUNITSKAYA[1]

[1]Kiev National University of Taras Shevchenko, Faculty of Chemistry, Department of Macromolecular Chemistry, 60 Vladimirskaya St, 01033 Kiev, Ukraine
[2]Institute for Macromolecular Chemistry, National Academy of Sciences of Ukraine, 48 Kharkovskoye Shosse, 02160 Kiev, Ukraine
[3]Institute of Botany, National Academy of Sciences of Ukraine, 2 Tereschenkovskaya St., 01601 Kiev, Ukraine

Block copolymers: MOPEO-b-PAAm and PAAm-b-PEO-b-PAAm contained poly(ethylene oxide), its monomethyl ether and chemically complementary polyacrylamide were and used as special matrices in the borohydride reduction of Ag^+ ions. Ag-nanoparticles in the structure of compositions were obtained. The effect of chemical nature, molecular architecture and size stabilization of silver nanoparticles in bulk structure was shown.

Keywords Silver nanoparticles; bulk structure; polymer matrices; triblock copolymer

Introduction

One of the actual aspects of the nanotechnology development is elaboration of the controlled synthesis methods of metal nanoparticles, which are active components of nanoscale electronics, photonics and sensorics [1–5]. The metal nanoparticle dispersions, mainly gold, silver and platinum group metal, were intensively studied [1,4,6]. These nanoparticles are perspective for bioanalytical electrochemistry, biodiagnostics, biomedicine and other purposes [7–9]. Although the synthesis and physical characterization of metal nanocrystals have been generally investigated, considerably less attention has been devoted to the fabrication of the novel nanostructured materials. In particular, a high chemical activity of zero-valent silver can cause the irreversible aggregation of Ag-nanoparticles that create the problem of their storage stability. To solve this problem, the development of nanoparticle synthesis methods in polymer matrices, which will provide the control of nanoparticle sizes and forms and also their stabilization in a solution, is necessary. In the recent years, many amphiphilic block copolymers, which form reversible micelles in an organic medium, were used to obtain the Ag-containing nanocompositions [10,11]. However, the great interest in terms of the use of silver nanoparticles is their synthesis in aqueous solution as well as

*Corresponding author, S. V. Fedorchuk. Tel.: +380442393411; Fax: +380442393100. E-mail: sergey_fedorchuk@ukr.net

Table 1. Molecular parameters of copolymers

Matrices	M_{nPEO}, кDa	M_{nPAAm}, кDa	$M_{nDBC/TBC}$, кDa	W_{PEO}, %	n
DBC	5	29.8	34.8	14.37	4
TBC	6	117.0	240.0	2.50	12

study the size and structure of the obtained metal-polymer compositions. Thus, this work is devoted to the study of morphological parameters such compositions.

Experimental

In the present work, we have synthesized asymmetric micelle-forming MOPEO-*b*-PAAm diblock copolymer (DBC) and PAAm-*b*-PEO-*b*-PAAm triblock copolymer (TBC) comprised methoxypoly(ethylene oxide) or poly(ethylene oxide) and chemically complementary polyacrylamide. We carried out syntheses of DBC and TBC using the template radical block and graft copolymerization, which was initiated by the Red/Ox reaction of cerium ammonium nitrate with hydroxyl groups of MOPEG and PEG [12,13]. Molecular parameters of polymer matrices are shown in Table 1.

These copolymers we used as special matrices in the process of borohydride reduction of Ag^+ ions in order to obtain stable silver nanoparticles.

The reduction of silver ions was carried out in aqueous polymer solutions with the eightfold molar excess of $NaBH_4$ that allowed achieving practically complete conversion of Ag^+ ions to zero-valent state in a selected region of $AgNO_3$ concentrations ($C_{AgNO3} = 1.82 \cdot 10^{-2}$ kg·m^{-3}) [14,15]. We used concentration of the polymeric matrices $C_m = 2.0$ kg·m^{-3}. The reagents were mixed in the deionized water. Polymeric solutions was mixed with $AgNO_3$ and kept for 30 min in a dark box; then the reducing agent was added. At the same time, borohydride anions participate also in some side reactions, due to which their essential excess is used to enhance the yield of Ag nanoparticles [14]. Also the reduce Ag nanoparticles without polymer matrix (test system) was investigated.

To determine the Ag-nanoparticle size and morphology as well as the bulk structure of the studied polymer-metal compositions, we used wide-angle and small-angle X-ray scattering (WAXS and SAXS) and transmission electron microscopy (TEM) [16,17]. Polymer-silver compositions were prepared from the reaction mixtures in Teflon forms by drying on air during 10 days and then in a vacuum desiccator.

WAXS profiles for the dried compositions were obtained in a cell with a thickness of 2 mm using a DRON-2.0 X-ray difractometer with Ni-filter in a primary beam. The monochromatic Cu-K_α radiation with $\lambda = 0.154$ nm, filtered by Ni, was provided by an IRIS M7 generator (at operating voltage of 30 kV and a current of 30 mA). The scattered intensities were measured by a scintillation detector scanning in 0.2° steps over the range of the $\theta = 3$–45° scattering angles (corresponding to $q = 2.13$–31.21 nm^{-1}, where $q = 4\pi \cdot \sin(\theta/2)/\lambda$ is the wavevector or the scattering vector). The diffraction curves obtained were reduced to equal intensities of the primary beam and equal values of the scattering volume [18]. Also, the normalization of experimental scattered intensities was carried out according to the (1) formula:

$$I_{n(i)}(\theta) = \left[I_{\exp}(\theta) - I_b(\theta)\right] \cdot (I/I_0) \quad (1)$$

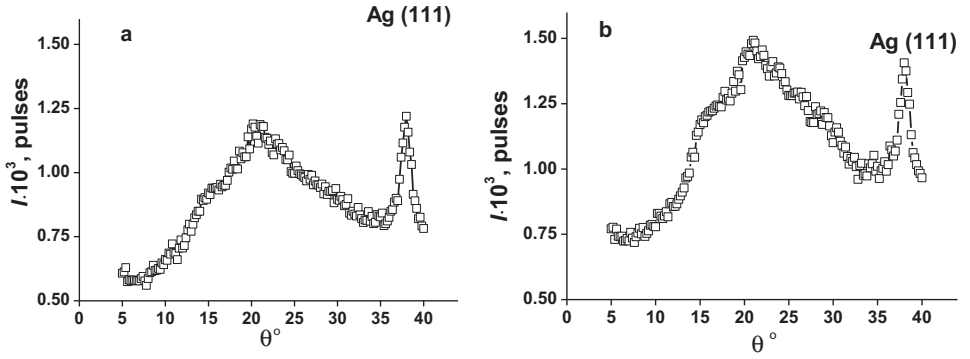

Figure 1. WAXS difractograms for the compositions: (a) DBC/Ag and (b) TBC/Ag. $T = 20^{\circ}$C.

where $I_{exp}(\theta)$ and $I_{n(i)}(\theta)$ are the experimental and normalized intensities in WAXS profile as a function of θ, $I_b(\theta)$ is the intensity of the background for every θ value, I_0 and I are the intensities of incident and scattered beams at $\theta = 0^{\circ}$ (the coefficient of the beam weakening).

SAXS profiles for the compositions were obtained in an automated Kratky slit-collimated camera. Here copper anode emission monochromated by total internal reflection and nickel filter was used. The intensity curves were recorded in the step-scanning mode of the scintillation detector in a region of the $\theta = 0.03$–4.0° scattering angles (the wavevector $q = 0.022$–2.86 nm^{-1}). Thus, the study of the micro-scale heterogeneous domains with characteristic dimensions (evaluated as $2\pi/q$) from 2 to 280 nm was possible. Normalization of SAXS profiles was carried out using the FFSAXS-3 program [18] and a standard sample from the laboratory of professor Kratky. The scattered intensities were normalized to the sample thickness and the scattered intensity of a standard. Additionally, the raw intensity curves were smoothed, corrected for parasitic scattering and desmeared.

TEM images of polymer/silver compositions were obtained with an electron microscope JEM-I23O from "JEOL" (Japan) at a voltage of 90 kV. Small drops ($\sim 1 \cdot 10^{-4}$ cm^3) of the compositions were placed on copper grids covered with Formvar film and carbon, and then quickly dried for 0.5–1 min at a room temperature.

Results and Discussion

The state of DBC and TBC in aqueous solutions was considered in our previous publications [19,20]. It was shown that asymmetric macromolecules of DBC and TBC formed the "hairy-type" micelles in aqueous medium due to interaction of MOPEO (PEO) and PAAm blocks followed by segregation (self-assembly) of non-polar bound parts. Relatively small "core" of these micelles contained non-polar bound parts of both the blocks but the developed "corona" comprised the segments of longer PAAm chains, which were unbound with PEO.

The process of nanoparticle formation was controlled by the changes in the position (λ_{max}) and the integral intensity (S) of the surface plasmon resonance band (SPRB), which was displayed in a visible region of spectrum [14]. More detail this experiment has been presented in previous works [21,22].

The results (Fig. 1, Table 2) showed that the bulk structure of the compositions contained a polymeric amorphous phase, that was displayed in WAXS profiles by two diffusive overlapped maxima at $\theta \sim 15^{\circ}$ and 21°, and crystalline Ag nanoparticles, that was confirmed

Table 2. Parameters of diffraction maxima in WAXS profiles of the compositions

	Position of the diffraction maximum			The average interplane distance		
Composition	θ_1, degrees	θ_2, degrees	θ_3, degrees	d_1, nm	d_2, nm	d_3, nm
DBC/Ag	~ 15.4	20.6	37.9	0.289	0.219	0.125
TBC/Ag	~ 15.7	20.9	37.9	0.284	0.216	0.125

by characteristic crystalline peaks of silver (111) at $\theta \sim 38^\circ$ [10]. The appearance of these peaks indicated the formation of crystalline Ag nanoparticles with tetragonal facet-centered cubic lattice [10]. An amorphous character of polymeric phases in the compositions was completely correlated with the data of WAXS studies [19,20], which demonstrated the loss of PEO crystalline properties in the block copolymer structure because of the interaction of the main and grafted chains i.e. IntraPC formation and existence of a glass transition in the structure of TBC.

As to the presence of two diffusive overlapped maxima in WAXS profiles in Fig. 1, they could be attributed (as in the study [19]) to the presence of two systems of planes of the paracrystalline lattice in the amorphous regions of PAAm-*b*-PEO-*b*-PAAm and MOPEO-*b*-PAAm structures, which contain mainly PAAm chains. The first maximum with smaller intensity at $\theta \sim 15^\circ$ characterizes the lateral periodicity in an arrangement of PAAm chains but the second one with greater intensity at $\theta \sim 21^\circ$ reflects the periodic arrangement of the flat hydrogen-bonded *cis*-dimers of amide groups in the structures of *cis-trans*-multimers [12]. It was note slight change in the position of the diffraction maximums for the polymer-metal compositions compared with individual block copolymer (~ 1) [12], apparently due to the presence in the structure of Ag nanoparticles.

The results of SAXS measurements in a form of the dependences of the scattered intensities versus q are shown in Fig. 2.

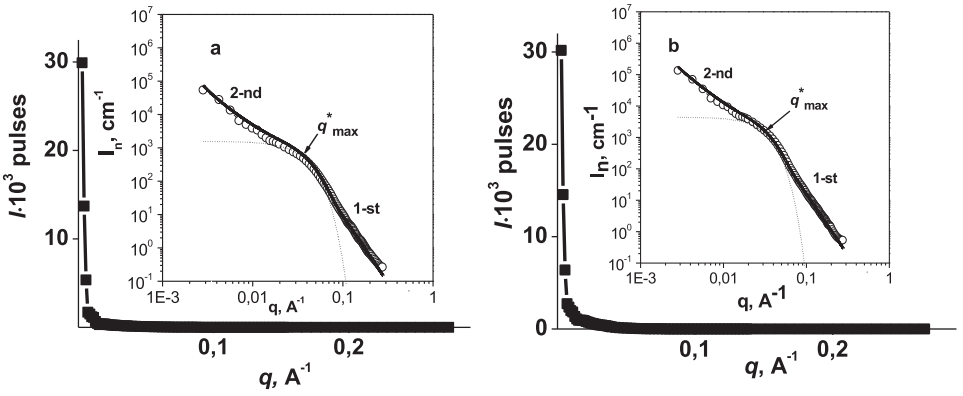

Figure 2. The intensity of small-angle X-ray scattering *vs* the wavevector for the compositions: (a) DBC/Ag and (b) TBC/Ag. The double logarithmic SAXS profiles are shown in a lesser scale; (a) = DBC/Ag, (b) = TBC/Ag.

All the profiles demonstrated a sharp fall in the scattered intensities with q growth (without any diffraction maxima) that pointed out the absence of any periodicity in the arrangement of structural elements of the compositions and polymer-inorganic hybrid at the supramolecular level. The same profiles in two logarithmic coordinates are exhibited in Fig. 2 in a lesser scale. Let's carry out their analysis from the point of view the fractal-cluster organization of the composition structure [23,24].

The double logarithmic SAXS profiles for the both compositions demonstrated two linear parts with different slopes, which corresponded to two power scattering regimes by Porod ($I \approx q^{-Df}$, where D_f is the slope ratio for corresponding straight line of log I *vs* log q). These linear parts were connected by the curve, which conformed to the exponential scattering regime by Guinier [23]. Such form of SAXS profiles in the double logarithmic coordinates pointed out the two-level fractal organization of a bulk structure of the compositions and polymer-inorganic hybrid. The character of separate elements of each level (the mass-fractal clusters, the surface-fractal clusters or solid particles with a smooth surface) could be determined by analysis of D_f value but the maximum diameter of these elements could be estimated by the relation $d_{max} \sim 2\pi/q^*$[18,23]. Finding the last parameter is possible in the case, when the straight line corresponding to the power scattering regime by Porod is ended (or "cuts") by the scattering regime by Guinier in the region of small q that is when a separate structural level is clearly displayed. A definite q^* value, which is determined in the region of the Guinier's scattering (Fig. 2) [23], is considered as "the cutting border." All said parameters (D_f, q^* and d_{max}) were established only for the 1-st lower level of structural organization of the compositions, which was displayed at higher q. For the 2-nd higher structural level, which was revealed at less q, only D_f numbers were found (Table 3) because corresponding straight lines of the Porod's scattering in Fig. 2 were not restricted from above by the Guinier's scattering regimes.

It is well known [23], that the $D_f = 4$ value characterizes the power scattering regime by Porod in the case of the dense solid scattering particles with a smooth surface. Exactly such values were determined for the linear parts of SAXS profiles, which corresponded to the 1-st structural level of the compositions (Table 3). This fact additionally confirmed the formation of the dense Ag nanoparticles in both the polymeric matrices. The maximum radius of a gyration for these particles was calculated using d_{max} value and the relation: $[R_g = d_{max}/2(5/3)^{1/2}]$ [23]. It turns out to be essentially less in the composition with MOPEO-*b*-PAAm (Table 3). Thus, the dense crystalline Ag nanoparticles constituted the 1-st level of the fractal-organized structure of the polymer-metal composites.

Using Beaucage's method of global unified exponential-power functions, [23,25], we modelled SAXS profiles for both compositions taking into consideration two levels of their

Table 3. Parameters of separate elements of the 1-st and 2-nd structural levels

System	DBC/Ag		TBC/Ag	
Value	1-st	2-nd	1-st	2-nd
D_f	4.0	2.2	3.9	2.2
$q^* \cdot 10^2$ / A^{-1}	3,9	—	2,8	—
d_{max} / nm	16,2	—	22,4	—
R_g / nm	6,3	—	8,7	—
$R_{g\ (calc)}$ / nm	5,0	—	6,0	—

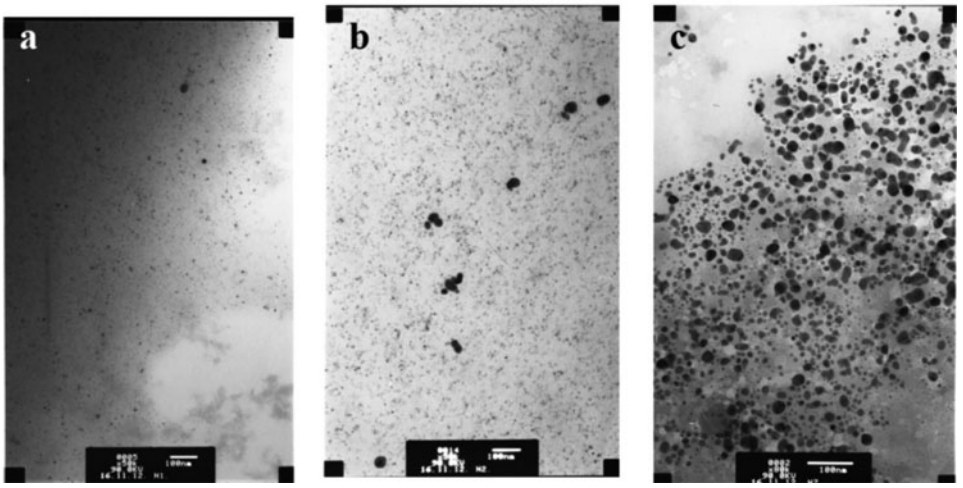

Figure 3. Electron micrograph of micellar structures MOPEO-*b*-PAAm/Ag (a), PAAm-*b*-PEO-*b*-PAAm/Ag (b) and test system without of polymer (c).

structural organization, which were discussed above. As a result, the value R_g (calc) for Ag-nanoparticles in the structure of compositions (Table 3) was obtained, which are well consistent with those that were found from the experimental profiles of SAXS, and was represented virtually the revised values of maximum hydrodynamic radius of the particles.

TEM images for both the compositions clearly demonstrated the presence of two types of Ag-nanoparticles in the polymer matrices. The majority of particles have relatively small size (2–10 nm), while isolated particle aggregates achieved 20–40 nm (Fig. 3).

It was found that the average size of Ag-nanoparticles obtained in MOPEO-*b*-PAAm micellar solutions (∼5 nm) turned out to be some less than that of the particles formed in PAAm-*b*-PEO-*b*-PAAm solutions (∼7 nm) (Fig. 3 a,b). This fact fully correlated with data of SAXS measurements and calculations represented in Table 3. The average dimension of separate Ag-nanoparticle aggregates was equalled to 30 nm according to represented TEM images. The formation of essentially larger Ag-nanoparticles (∼30 nm) was observed in the test system that is in pure water. Thus, the high stabilizing activity of both the block copolymers with respect to small Ag-nanoparticles is fully proved.

Conclusion

Block copolymers PAAm-*b*-PEO-*b*-PAAm and MOPEO-*b*-PAAm, which form Intra PCs and self-assemble in micellar structures in aqueous solutions, could be considered as efficient nanoreactors. They are capable of ensuring the high rate and efficacy of the borohydride reduction of silver ions up to the stable crystalline Ag nanoparticles with $R_g \sim 5$–6 nm. The compositions of PAAm-*b*-PEO-*b*-PAAm and MOPEO-*b*-PAAm with Ag nanoparticles showed the two-level fractal organization of their structure. The dense crystalline silver nanoparticles were the separate elements of the 1-st lower level, while the mass-fractal clusters of the polymeric matrices constituted the 2-nd higher structural level. The formation of smaller silver nanoparticles under the influence DBC ($R_g = 5$ nm) compared to TBC (Rg = 6 nm) was found.

References

[1] Manna, A., Imae, T., Aoi, K., Okada, M., & Yogo, T. (2001). *Chem. Mater.*, *13*, 1674.

[2] Wilson, O. M., Scott, R. W. J., Garcia-Martinez, J. C., & Crooks, R. M. (2004). *Chem. Mater.*, *16*, 4202.

[3] Porel, S., Singh, S., Harsha, S. S., Rao, D. N., & Radhakrishnan, T. P. (2005). *Chem. Mater.*, *17*, 9.

[4] Huber, K., Witte, T., Hollmann, J., & Keuker-Baumann, S. (2007). *J. Am. Chem. Soc*., *129*, 1089.

[5] Sohn, B. H., Choi, J. M., Yoo, S., Yun, S. H., Zin, W. C., Jung, J. C., Kanehara, M., Hirata, T., & Teranishi, T. (2003). *J. Am. Chem. Soc*., *125*, 6368.

[6] Xu, H., Xu, J., Zhu, Z., Liu, H., & Liu, S. (2006). *Macromolecules*, *39*, 8451.

[7] Kittler, S., Greulich, C., Köller, M., & Epple, M. (2009). *Mat.-wiss. u. Werkstofftech*., *40*, 258–264.

[8] Schmid, G. (2004). *In: Nanoparticles: From theory to application*. Wiley–CH Verlag GmbH & Co: Weinheim, 444.

[9] Zlem, O., Kalayci, A., Sun, F., Comert, B., Hazer, B., Atalay, T., Cavicchi, K. A., & Cakmak, M. Polym. (2010). *Bull*., *65*, 215.

[10] Becturov, E. A., Kudaybergenov, S. E., Garmagambetova, A. K., Iskakov, R. M., Ibraeva, J. E., & Shmakov, S. N. (2010). *Polymer-protected metal nanoparticles: Almaty*, 274.

[11] Horikoshi, S., Abe, H., Torigoe, K., Abe, M., & Nick (2010). *Serpone, Nanoscale*, *2*, 1441.

[12] Zheltonozhskaya, T., Permyakova, N., & Momot, L. (2009). in: V. V. Khutoryanskiy, G. Staikos, *Hydrogen-Bonded Interpolymer Complexes. Formation, Structure and Applications Chapter 5*, World Scientific: New Jersey-London-Singapore-Beijing etc.

[13] Zheltonozhskaya, T. B., Fedorchuk, S. V., & Syromyatnikov, V. G. (2007). *Russ. Chem. Rev.*, *76*, 731.

[14] Sergeev, B., Lopatina, L., Prusov, A., & Sergeev, G. (2005). *Colloid. J*., *67*, 79.

[15] Maltceva, N. N., *et al*. (1985). *Sodium borohydride. Characteristic and application Nauka*, Moscow, Ru.

[16] Alexandridis, P. (2000). in: P. Alexandridis, B. Lindman. *Self-Essembly and Applications*. Elsevier: Amsterdam, 1, 435.

[17] Chung, T. C. (2002). *Prog. Polym. Sci*., *27*, 39–85.

[18] Lipatov, Yu. S., Shilov, V. V., Gomza, Yu. P., *et al*. (1982). *X-Ray Diffraction Methods to Study Polymeric Systems Nauk*. Dumka, Kyiv Ua.

[19] Fedorchuk, S. V., Zheltonozhskaya, T. B, Permyakova, N. M., Gomza, Y. P., Nessin, S. D., & Klepko, V. V. (2008). *Mol. Cryst. Liq. Cryst*., *497*, 268.

[20] Fedorchuk, S. V., Zheltonozhskaya, T. B., Shembel, E. M., Kunitskaya, L. R., Maksuta, I. M., & Gomza, Y. P. (2011). *Func. Mat*., *18*, 1.

[21] Fedorchuk, S., Zheltonozhskaya, T., Gomza, Yu., Nessin, S., Kunitskaya, L., & Demchenko, O. (2011). *Mac. Symp*., *317–318*, 103.

[22] Fedorchuk, S. V., Zheltonozhskaya, T. B., Gomza, Yu. P., Nessin, S. D., & Kunitskaya, L. R. (2012). *Proc. of the Intern. Conf.* Nanomaterials: Applications and Properties, *1*, 1.

[23] Shpak, A. P., Shilov, V. V., Shilova, O. A., & Kunitskiy, Yu. A. (2004). *Diagnostics of nanosystems., Multilevel fractal structures Nauk*. Dumka, Kyiv, Ua.

[24] Zhang, F., & Ilavsky, J. (2010). *J. Macromol. Sci*., *50*, 59.

[25] Beaucage, G., Hyeonlee, J., Pratsinis, S., & Vemury, S. (1998). *Langmuir.*, *14*, 5751.